Title
Sensitivity of GRETINA position resolution to hole mobility

Authors
Prasher, VS
Cromaz, M
Merchan, E
et al.

Publication Date
2017-02-01

DOI
10.1016/j.nima.2016.11.038

Peer reviewed

Sensitivity of GRETINA position resolution to hole mobility

V.S. Prasher[1], M. Cromaz[2], E. Merchan[1], P. Chowdhury[1,*], H.L. Crawford[2], C.J. Lister[1], C.M. Campbell[2], I.Y. Lee[2], A.O. Macchiavelli[2], D.C. Radford[3], A. Wiens[2]

[1] *Department of Physics, University of Massachusetts Lowell, Lowell, MA 01854, USA*
[2] *Nuclear Science Division, Lawrence Berkeley National Laboratory, Berkeley, CA 94720, USA*
[3] *Physics Division, Oak Ridge National Laboratory, Oak Ridge, TN 37831, USA*

Abstract

The sensitivity of the position resolution of the gamma-ray tracking array GRETINA to the hole charge-carrier mobility parameter is investigated. The χ^2 results from a fit of averaged signal ("superpulse") data exhibit a shallow minimum for hole mobilities 15% lower than the currently adopted values. Calibration data on position resolution is analyzed, together with simulations that isolate the hole mobility dependence of signal decomposition from other effects such as electronics cross-talk. The results effectively exclude hole mobility as a dominant parameter for improving the position resolution for reconstruction of gamma-ray interaction points in GRETINA.

Keywords: `hole mobility, basis, signal decomposition, HPGe detectors, γ-ray tracking`

1. Introduction

The high-resolution gamma-detection arrays of the previous generation used individual hyper-pure germanium (HPGe) crystals that were housed in scintillator envelopes for Compton suppression. While necessary to provide good peak-to-total, this arrangement limited the HPGe solid angle coverage of the array to $< 50\%$ and, consequently, the overall photo-peak efficiency for the instrument. The next-generation devices advancing current frontiers of nuclear spectroscopy are eliminating the low-resolution scintillator envelopes entirely and consist of a 4π HPGe shell. The individual crystals have electrically segmented outer contacts which can be used to reconstruct gamma-ray interaction points with $\sigma \sim 2$mm RMS resolution [1],[2]. This position sensitivity is necessary to allow gamma-ray tracking through the HPGe volume, which enables the identification of gamma-rays that did not deposit their full energy in the detector. The Gamma Ray Energy Tracking In-beam Nuclear Array (GRETINA) is the first stage of a planned full 4π Gamma Ray Energy Tracking Array (GRETA) [3] in the US, with a similar device AGATA [4] being constructed in Europe.

The geometry and operating principles of the GRETINA detector modules have been described in earlier publications [1, 5, 6]. The 3-D position reconstruction of the gamma-ray interaction points in these coaxial HPGe detectors relies on direct charge measurements of electrons and holes collected at the central and outer-segment contacts, respectively, as well as image charges that are induced in neighboring segments. In general, the drift time of the net charge in the hit segment is sensitive to the radial position of the interaction point while the image charges in the nearby segments help in constraining the other two coordinates, namely the depth

*Corresponding author.

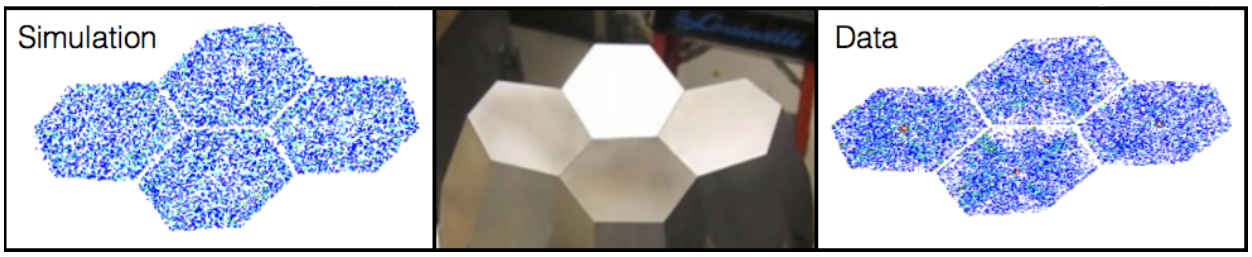

Figure 1: Middle panel shows a single GRETINA quadruple crystal cryostat (Photo courtesy of Mirion Technologies (Canberra) - Lingolsheim Facility). Left and right panels shows the inferred interaction points for simulated (left) and experimental data, determined from the signal decomposition algorithm (right) for ^{137}Cs source, respectively, and restricted to the first 2cm of depth for both the simulation and experiment.

and azimuthal angle [7]. In practice, while signal traces from *all* segments are collected, the signal decomposition algorithm compares direct and induced signals from only the net charge segment and its nearest neighbors in a single crystal to a unique pre-determined "crystal basis" of pulses (see Section 2.1) to extract positions of gamma-ray interactions. This basis is generated from a simulation of net and induced charges on the detector contacts as a function of time, for a unit charge drifted in the detectors electric field, starting from each position on a grid of points which span the detector volume. Multiple interaction points for an individual gamma ray are extracted from the experimental pulses through a signal decomposition process by comparing them to a superposition of signals generated from multiple interaction points in the simulated basis. The success of signal decomposition, and thus ultimately the tracking algorithms, depends crucially on the accuracy of this basis in reproducing experimental signals. The fidelity of the simulated crystal basis depends on a number of parameters, such as the electric field, the weighting potentials for each segment (which define the degree of coupling of a charge at a given position to a given electrode [8], and is used in calculating the induced signal through the Shockley-Ramo theorem [9, 10]), as well as the impurity concentration and mobilities of the charge carriers in the medium. Corrections to the basis signals are also included for electronics effects such as cross-talk between neighboring segments and rise-time shaping, in order to produce a dependable simulated basis of responses to an array of discrete interaction points, which serves as input for signal decomposition in tracking algorithms.

GRETINA, the 1π array consisting of 28 hexagonal crystals arranged in 7 quad cryostats, has been commissioned and has met its performance goal with first hit position resolution (σ = 2mm RMS) [11]. Challenges still remain, however, in the unambiguous reconstruction of interaction points. This issue is best illustrated by comparing simulations to experimental data for events in a four-crystal quad unit shown in Figure 1 (middle) illuminated by a ^{137}Cs source. Simulations using GEANT4 [12], are shown in Figure 1 (left), where the interaction points in the x-y plane are seen to be evenly distributed in space with no obvious irregularities. The same exercise for actual experimental data, shown in Figure 1 (right), reveals a clustering of reconstructed events, especially near segment boundaries [13].

Improvements are necessary at the signal decomposition level. The signal generation and pulse shapes in the detector contacts depend on a thorough knowledge of a number of parameters in the material science domain, including charge carrier mobilities, impurity distributions, and drift velocity anisotropies along different crystal axes for both electrons and holes. For germanium, the proper-

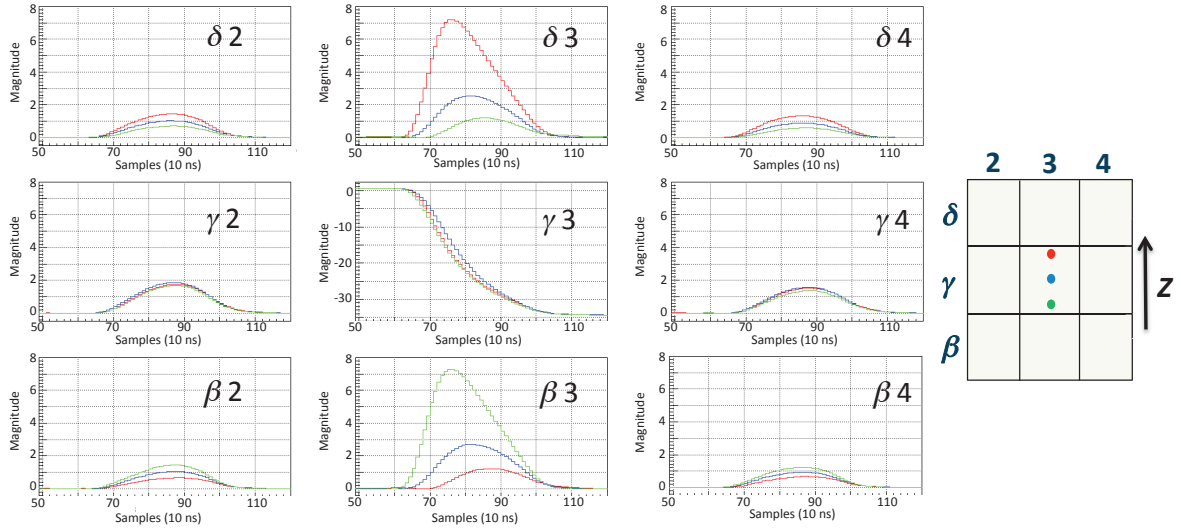

Figure 2: Examples of simulated charge signals corresponding to three different interaction positions in segment 3 of a 36-fold HPGe GRETINA detector. For each interaction position, the net charge signals from contact $\gamma 3$, corresponding to a fully absorbed γ ray, and the respective transient charge signals induced on the eight adjacent segments are shown. [Note: The schematic of the segments on the right is not to scale. In reality, the geometry of the segments is very different between the azimuthal and longitudinal directions, leading to different induced signal amplitudes.]

ties of hole mobilities are the least-well understood. This work explores the sensitivity to charge transport parameters, in particular hole mobilities, in the signal decomposition algorithm for GRETINA.

2. Pulse shape calculations

Drift velocity is a critical parameter in the charge collection and signal generation process in semiconductor materials. Drift velocity anisotropy can cause considerable differences in pulse shape rise time depending on the spatial position of the charge carrier creation. Experimentally, the dependence of pulse shapes on the electron drift velocity anisotropy in closed-end HPGe detectors has been clearly established [14], as well as its influence on tracking algorithms [15]. Anisotropy in the drift velocity for holes is also a major concern when dealing with semi-conducting devices operating at high-electric fields, where deviation from low-field ohmic behavior is observed [16].

To study how variations in hole mobility affect signal decomposition and, hence position resolution, calculations of the pulse shape, or electric charge induced at the electrodes were performed in the present work. One specific crystal of GRETINA, Q4A8 (an A-type crystal in the fourth quad module Q4, as explained in Ref. [1]), was used as a model in the simulations. The (n-type) crystal is a partially tapered irregular hexagon (8 cm diameter, 9 cm length, around 10° tapering angles) with a 36-fold segmentation on the outer p^+ ion-implanted contact. The central contact (1 cm diameter) is not segmented, is n^+ lithium diffused, and biased at +5 kV [5]. Depending on the radial position where the charge carriers are produced, they will have different drift paths to the electrodes. Therefore, the shapes of the transient image (in-

duced current) pulses are also different for different interaction positions. The shape and size of the signals contains the information on the 3-D position of and the energy deposited in each individual interaction within the Ge volume, as shown in Figure 2.

2.1. Raw basis

To extract position information, the experimentally measured pulse shapes are compared to a set of pulse shapes, termed a basis, which are calculated on a grid of points spanning the detector volume. The calculation of a basis is performed by using a suite of software codes, starting from the crystal geometry and properties as input and ending with the expected pulse shapes at each of the detector contacts [17]. The electric field inside the detector and the weighting potential for each outer segment contact are calculated on a non-linear grid with average spacing of 1 mm using the `fieldgen` software code [18], where both geometry and material properties of the detector are carefully incorporated, including the space charge density profile provided by the detector manufacturer. The non-linear basis point distribution is weighted to locations where the gradient of the weighting potential is steeper, i.e. where the signals change more rapidly with distance. The electric field is then used to calculate the drift path of electrons and holes from a given initial position on the grid by using the velocity (v) relation:

$$v(E(r)) = \mu(T, E(r), \varepsilon, \vartheta)E(r). \qquad (1)$$

The charge carrier mobility μ is not only a function of the temperature (T) and electric field (E) but also depends on the angle between the drift direction and the crystal orientation (ε) and the angle between the electric field and the crystal orientation (ϑ). The detailed parameters are discussed in section 2.2. In this calculation, the electric field is interpolated between the grid points, with a small enough time interval (e.g. 2 ns) to prevent discontinuities in the drift velocity. Once the drift path is established, the net and transient currents induced on each of the 36 segment contacts, and on the central contact, for a unit charge created at the initial position are calculated using the `siggen` software code [19]. The full set of these calculations forms a raw basis which is subsequently corrected for electronic effects as described in Section 3.1.

2.2. Drift velocities

The conductivity of Ge is anisotropic, i.e. the mobility of electrons and holes varies depending on the direction of the applied electric field with respect to the lattice vectors. Most prior experimental results on drift velocities are based on the measurement of the time required by electrons or holes created by ionizing radiation to traverse a known thickness of sample under the effect of an applied electric field [2, 16, 20, 21, 22, 23]. These techniques yield mobility parameters that do not include hole trapping and de-trapping effects, which are present in real detectors [24].

Assuming knowledge for the drift velocity of electrons and holes (either measured or calculated) along the three major Ge crystal axes, the drift velocities for an arbitrary field direction are calculated and used to create the pulse shapes in the raw GRETINA basis. This model also includes the temperature dependence of the drift velocities, which decrease at higher temperatures due to increased scattering with the lattice vibration [25]. Drift velocities for electrons and holes in high-purity Ge have been deduced for a range of relevant temperatures ($77 \leq \mathrm{T} \leq 100$°K) and electric fields ($1 \leq \mathrm{E} \leq 5000$ V/cm) applied parallel to $\langle 100 \rangle$, $\langle 110 \rangle$, $\langle 111 \rangle$ crystallographic directions [26].

The reliability of the techniques from which the current GRETINA parameters are derived depends not only on the precision with which the simulations are performed but also upon the basic knowledge

of the Ge band structure and the different scattering mechanisms which determine charge carrier motion. In contrast to electrons, no direct description of the anisotropic mobility for holes exists in the literature. This is due to the complex nature of the valence band in germanium [27, 28]. While an exact determination of hole mobility parameters is outside the realm of the present work, an alternate approach to optimize these parameters for a GRETINA detector is presented here.

3. Current Approach

3.1. The superpulse method

The averaged signals for each crystal electrode, 36 segments and one core, can be concatenated and presented as a single pulse train called a "superpulse". The superpulse method in GRETINA was introduced as a way to derive electronic response corrections for the calculated basis signals. These corrections are determined by comparing measured superpulses from a ^{60}Co source measurement to the averaged signals from simulation, and performing a least-squares fit of parameters that model the electronic response of the the detector. These parameters include integral and differential crosstalk between segments, as well as delays and preamplifier shaping. The extracted parameters are then applied to the raw basis defined in Section 2.1, to obtain a basis corrected for detector responses.

In the present work, we attempted to optimize the charge drift velocity parameters by adjusting the hole mobility in the calculated basis and minimizing the χ^2 to the superpulse data (which is subsequently used to extract detector response parameters). The relative mobilities along the different axes, which can be measured through azimuthal variation in drift times in a cylindrical detector and calculated through Monte-Carlo methods, are better determined than are the overall mobilities. Therefore, all hole mobilities were scaled together over a range varying from 30% lower to 30% higher than the currently adopted values, in 5% steps, and raw bases were created for each step in this range (Figure 3 shows the adopted hole mobility curves currently used in GRETINA, and those used for the ±15% analysis).

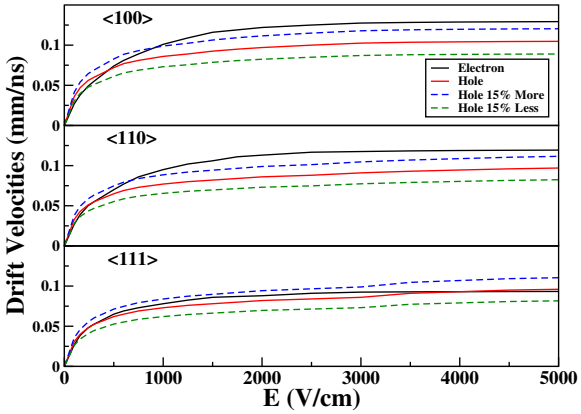

Figure 3: Solid lines shows the drift velocities of electrons and holes along the three principal Ge crystal axis (<100>, <110>, <111>) as a function of the electric field, as currently used for GRETINA [26]. The dashed lines show hole velocities varied by ±15% from currently used values.

A complication arises in that the parameters involved in the superpulse fitting procedure are not truly independent. The preamplifier shaping time, τ, in particular, is correlated with hole mobility. This is evident from Figure 4, where the average τ value for all segments is seen to track the change in hole mobility, if allowed to vary independently in fitting observed signal pulse shapes. For fitting a given pulse shape, increasing hole mobility speeds up charge collection, which can be offset by a slower (or longer) preamplifier shaping time, in minimizing χ^2. Thus, in order to extract the specific effect of hole mobility changes, constrained fits were performed with the pre-amplifier response rise time parameters fixed. The results for χ^2, as shown in Figure 5, indicate a shallow minimum centered around hole mobilities that are ≈15% lower than currently used values (see Section 2.2).

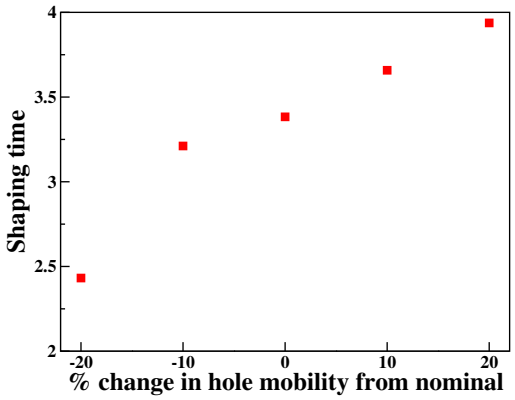

Figure 4: Average preamplifier shaping time as a function of hole mobilities around currently used values.

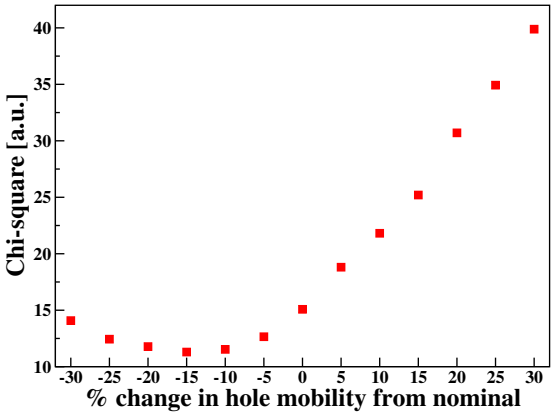

Figure 5: χ^2 results for the fit of experimental superpulses with simulated superpulses, as a function of the hole mobilities change (%) from the currently adopted values. Since the noise in the averaged superpulses is not well defined, the values of χ^2 have an arbitrary normalization factor.

3.2. Experimental pencil beam studies

While the minimum χ^2 in the superpulse fitting procedure may suggest that hole mobilities be decreased by ≈15% from currently adopted values, the real test of an optimized parameter set lies in the achieved experimental position resolution of the detector. To that end, the position resolution of a GRETINA detector (Q4A8) using current hole mobilities was compared to the resolution obtained analyzing the same raw data, but assuming 15% lower hole mobilities.

Data from a collimated 2 mm diameter "pencil" beam of 662 keV γ rays from a ^{137}Cs source was analyzed. The scatter of inferred first interaction points about the photon beam direction from the collimated source provides an experimental measure of the position resolution. The ^{137}Cs beam was collimated to enter the Q4A8 detector front face at specific locations as shown in Figure 6. The black circles indicate 7 different collimator locations. Five of these were spaced to enter the crystal at radial distances of 6, 12, 17, 22 and 30 mm from the symmetry axis of the detectors at a fixed x position of zero in the coordinate system shown. To explore azimuthal variations, two additional locations at a fixed y position of 12 mm were chosen at x positions of -3.5 and -7.5 mm.

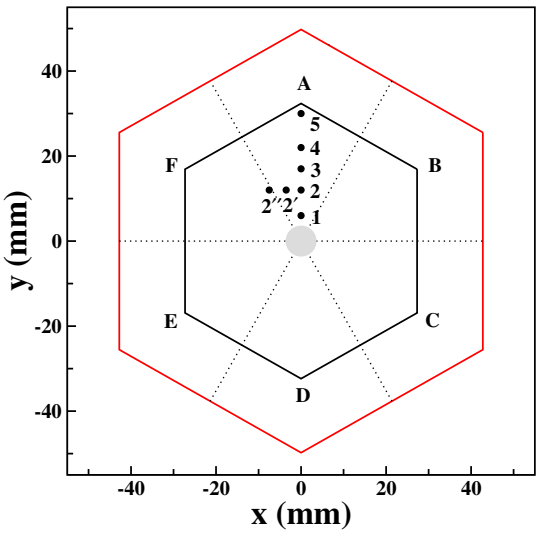

Figure 6: Pencil beam collimation points used for the position sensitivity measurement (Q4A8 GRETINA detector). The inner hexagon defines the front face. The segments are labeled A-F in azimuthal direction and the dashed lines indicates the segment boundaries. Black dots indicate 7 different collimator locations, where the pencil beam measurements were carried out.

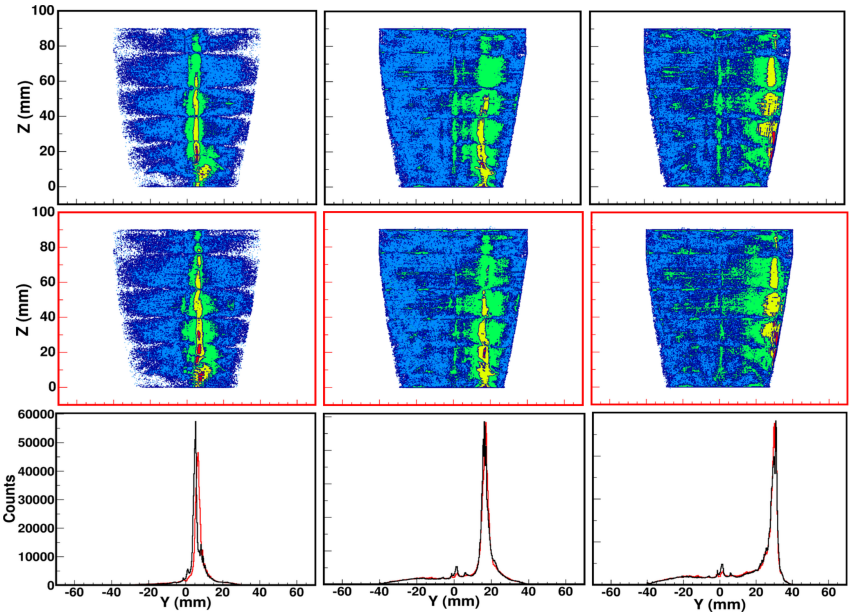

Figure 7: The upper panel shows 2D y-z histograms for three different experimental pencil beams (from left: 1, 3, 5 collimation points) with current hole mobility parameters, with an imposed requirement of a single segment hit. The middle panel shows corresponding 2D plots with 15% lowered parameters. The overlaid projections in the lower panel are y-projections for the two different mobilities, where color corresponds to their respective 2D picture frame.

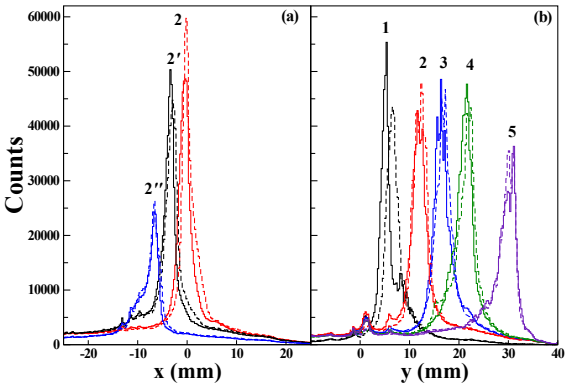

Figure 8: Comparison of (a) x-projections for the azimuthal points 2, 2' and 2", and (b) y-projections for all the radial points 1-5, between current (solid lines) and 15% lower (dashed lines) hole mobility parameters.

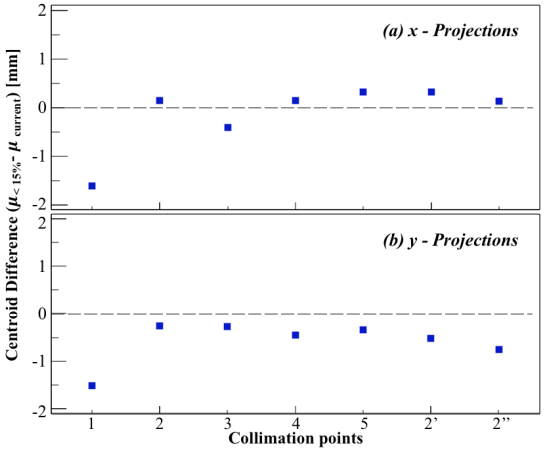

Figure 9: Difference of pencil beam (a) x-projection and (b) y-projection centroids for all the pencil beam collimation points along the radial and azimuthal lines. The shift on the y axis is defined as the centroid with the hole mobility μ decreased by 15% minus the centroid assuming the nominal value of hole mobility.

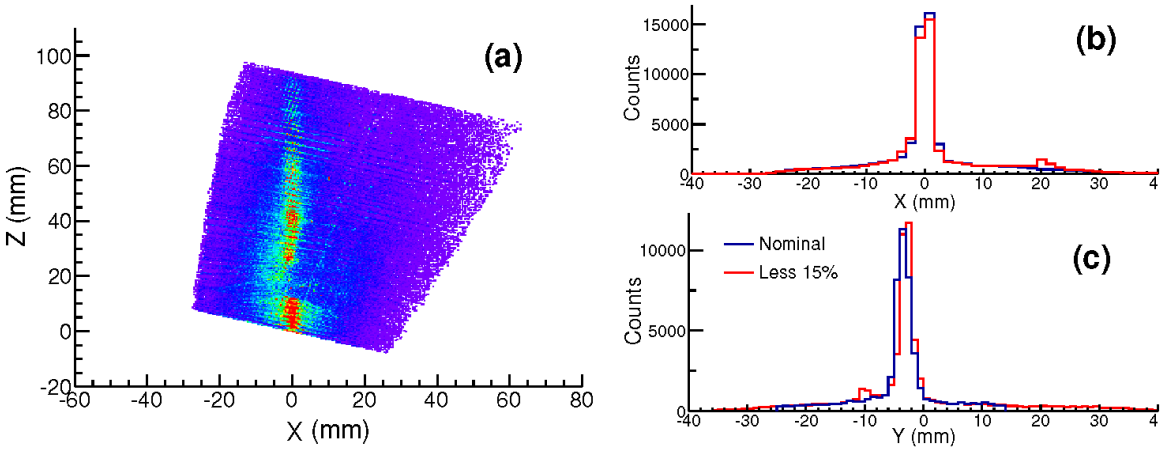

Figure 10: (a) 2D histogram (x-z) of a simulated pencil beam with the current hole mobility parameters used for the signal decomposition. The projections of the (b) x and (c) y dimensions of the pencil beam as defined by Figure 10(a) for the nominal, or current hole mobility parameters (blue) and the 15% lower hole mobility parameters (red).

Ideally, coincidence scanning techniques can provide a well-defined single scatter interaction position in the crystal in all 3 dimensions. In the absence of such a data set, for the present work in order to determine the position, two conditions are imposed on the events considered: (a) they are limited to a single interaction points as determined by the decomposition algorithm, and (b) the energy of this interaction is required to be greater than 300 keV. The y-position resolutions obtained for the two different hole mobilities are shown for three radially varying points in Figure 7. The collimation of the source is clearly evident in the two-dimensional y vs z plots. The requirement of a single segment hit reduces the likelihood of events at the segment boundary due to charge-sharing. For all but point 1, there is no significant difference observed in the y position profiles obtained with the two different hole mobilities. This becomes more evident from Figure 8, where the x-projections for the three azimuthal points 2, 2' and 2", and y-projections for all the radial points 1 to 5 are shown. A quantitative comparison of the x-y centroid shifts of the reconstructed peaks is shown in Figure 9. Point 1 stands out, with a shift of ∼1.5 mm between the two hole mobilities; the typical FWHM of the position distributions is ∼4 mm.

The fact that point 1 is the single data set among the collimation points that exhibits a significant dependence on hole mobilities can be understood from the fact that it is the closest point to the central contact. Therefore, holes, which move away from the central axis, have to travel the farthest distance to the outer electrodes for point 1. Based on this observation, one can conclude that the detector volume for which a 15% change in hole mobility would result in a significant shift in position (or change in position resolution) is just a small fraction of the total active detector volume, located near the central contact.

3.3. Simulations of pencil beams

To ensure that the above observations from the experimental pencil beam for varying hole mobilities are inherent in the data, and are not artifacts of the analysis procedure itself, the same position reconstruction algorithm was tested on a simulated pencil beam data set, which is free from the electronic effects observed in data.

A GEANT4 simulation [12] was used to generate interaction positions for a collimated ^{137}Cs source in a single detector volume, replicating fully the experimental setup with a 2 mm diameter collimation, positioned at $x = 0$ mm and $y = 6$ mm at the front face of the crystal. These positions were then used to create a set of simulated "raw" data, using the basis signals calculated using the currently adopted hole mobilities, and constructing the required linear superposition of signals for each simulated event. These "raw" data were analyzed using the same signal decomposition codes as used for the experimental data, with the decomposition being performed with both the basis with standard hole mobilities and a basis calculated using hole mobilities modified to be 15% lower than the adopted values.

In the simulated data, there is no difference in position resolution between the two hole mobilities that differ by 15%, either in the x or y dimensions as defined by Figure 10(a) (Figure 10(b) and (c)). In addition, there is no statistically significant shift in the centroid in the simulated pencil beam, even though the pencil beam is quite close to the core.

Thus, while the χ^2 minimization from the superpulse fitting procedure indicates a shallow minimum centered at hole mobility values 15% lower than currently in use, the determination of the interaction positions seems fairly insensitive to a 15% variation in hole mobilities, both for experiment and simulation. It seems that at this point, the adopted GRETINA hole mobility is not limiting position resolution, and future efforts to improve position reconstruction should focus on other parameters such as, for example, electronic cross-talk, field non-uniformity, correlated noise or the crystal impurity distribution. Of these, field non-uniformity is perhaps the most important, especially close to segment boundaries, where the charge cloud size generated by the interactions may be an issue as they change the signal shape.

4. Conclusions

The position resolution for the determination of γ-ray interaction points is a key metric in the performance of the GRETINA spectrometer, as it strongly affects the fidelity and efficiency for downstream data analysis. This has a strong impact on improving the overall efficiency and peak/total ratios. It also determines the effective energy resolution of the array when used with gamma-ray sources with high recoil velocities, where corrections for Doppler shifts are critical. While a number of parameters may affect the ultimate position resolution, this work specifically explored whether variation in the hole charge carrier mobility parameters, which are not well determined experimentally, is a significant contributor.

When the sensitivity of variation of hole mobilities was examined using averaged signals via the superpulse method, the χ^2 fits exhibited only a shallow minimum as a function of the hole mobility, centered at $\approx$15% less than currently adopted values in GRETINA. However, when a 15% reduction in hole mobilities is applied to the analysis of experimental data taken using collimated sources, no appreciable impact is observed. Thus, hole mobilities appear to be largely optimized and are not currently limiting position resolution. These results, therefore, exclude hole mobility as a dominant parameter for addressing remaining challenges in reconstructing gamma-ray interaction points in GRETINA.

This work is supported by the U.S. Department of Energy, Office of Science, Office of Nuclear Physics, under award number DE-FG02-94ER40848 and contract numbers DE-AC02-05CHI1231 (LBNL) and DE-AC05-00OR22725 (ORNL). GRETINA was funded by the U.S. DOE Office of Science. Operation of the array is supported by the DOE under Grand No. DE-AC02-05CH11231 (LBNL).

References

[1] S. Paschalis *et al.*, Nucl. Instr. and Meth. A **709**, 44 (2013).
[2] B. Bruyneel *et al.*, Eur. Phys. J. A **52**, 70 (2016).
[3] I.-Y. Lee, Nucl. Phys. A **834**, 743c (2010).
[4] S. Akkoyun *et al.*, Nucl. Instr. and Meth. A **668**, 26 (2012).
[5] K. Vetter *et al.*, Nucl. Instr. and Meth. A **452**, 105 (2000).
[6] M. Descovich *et al.*, Nucl. Instr. and Meth. A **553**, 535 (2005).
[7] K. Vetter *et al.*, Nucl. Instr. and Meth. A **452**, 223 (2000).
[8] E. Gatti *et al.*, Nucl. Instr. and Meth. **193**, 651 (1982).
[9] W. Shockley, J. Appl. Phys. p. 635 (1938).
[10] S. Ramo, Proc. IRE **584**, 39 (1939).
[11] M. Cromaz, J. Phys.: Conf. Series **606**, 012016 (2015).
[12] L. A. Riley, UCGretina GEANT4, Ursinus College (unpublished) (2014).
[13] V. S. Prasher, PhD Thesis, U. Massachusetts Lowell, MA, USA (2015).
[14] L. Mihailescu *et al.*, Nucl. Instr. and Meth. A **447**, 350 (2000).
[15] I. Abt *et al.*, Eur. Phys. J. C **68**, 609 (2010).
[16] E. J. Ryder, Phys. Rev. **90**, 766 (1953).
[17] T. Kröll *et al*, Nucl. Instr. and Meth. A **463**, 227 (2001).
[18] *http://radware.phy.ornl.gov/gretina/fieldgen* (2006).
[19] *http://radware.phy.ornl.gov/gretina/siggen* (2006).
[20] M. B. Prince, Phys. Rev. **92**, 681 (1953).
[21] L. Reggiani *et al.*, Phys. Rev. B **16**, 2781 (1977).
[22] J. P. Nougier *et al.*, Phys. Rev. B **8**, 5728 (1973).
[23] M. Schlarb *et al.*, Eur. Phys. J. A **47**, 132 (2011).
[24] R. Trammell *et al.*, Nucl. Instr. and Meth. **76**, 317 (1969).
[25] M. Ali Omar *et al.*, Solid-State Electronics **30**, 1351 (1987).
[26] I.-Y. Lee, GRETINA Technical Note: Electron and Hole Drift Velocity in Ge, Document GRT-6-061112 (2006).
[27] W. Fawcett, Proc. Phys. Soc. **85**, 931 (1965).
[28] C. Jacoboni *et al.*, Phys. Rev. B **24**, 1014 (1981).